Electrochemical Biosensor of Nanocube-Augmented Carbon Nanotube Networks

Jonathan C. Claussen,[†,‡] Aaron D. Franklin,[†,§] Aeraj ul Haque,[⊥,¶] D. Marshall Porterfield,[⊥,¶] and Timothy S. Fisher[†,‡,*]

[†]Birck Nanotechnology Center, [‡]School of Mechanical Engineering, [§]School of Electrical and Computer Engineering, [⊥]Department of Agricultural and Biological Engineering, and [¶]Bindley Bioscience Center-Physiological Sensing Facility, Purdue University, West Lafayette, Indiana 47907

ABSTRACT Networks of single-walled carbon nanotubes (SWCNTs) decorated with Au-coated Pd (Au/Pd) nanocubes are employed as electrochemical biosensors that exhibit excellent sensitivity (2.6 mA mM^{-1} cm^{-2}) and a low estimated detection limit (2.3 nM) at a signal-to-noise ratio of 3 (S/N = 3) in the amperometric sensing of hydrogen peroxide. Biofunctionalization of the Au/Pd nanocube-SWCNT biosensor is demonstrated with the selective immobilization of fluorescently labeled streptavidin on the nanocube surfaces *via* thiol linking. Similarly, glucose oxidase (GOx) is linked to the surface of the nanocubes for amperometric glucose sensing. The exhibited glucose detection limit of 1.3 μM (S/N = 3) and linear range spanning from 10 μM to 50 mM substantially surpass similar CNT-based biosensors. These results, combined with the structure's compatibility with a wide range of biofunctionalization procedures, would make the nanocube-SWCNT biosensor exceptionally useful for glucose detection in diabetic patients and well suited for a wide range of amperometric detection schemes for clinically important biomarkers.

KEYWORDS: carbon nanotubes · glucose biosensor · nanoparticles · nanocubes · fluorescence

Detection of biomolecules at low concentrations is critically important to the early diagnosis and successful treatment of diseases.[1,2] Electrochemical biosensors developed with nanomaterials offer highly sensitive, real-time detection of clinically important analytes with low power requirements for decentralized testing in remote locations.[3−6] For example, single-walled carbon nanotubes (SWCNTs) have enabled improvements such as (1) increased sensitivity in enzymatic electrochemical biosensors because of their inherent electrocatalytic activity toward the oxidation of hydrogen peroxide (H_2O_2) and NADH[7] and (2) amplification of the electrochemical signal in nucleic acid biosensors[8] and cancer biomarker immunosensors.[9] Recently, nanomaterials, from SWCNT arrays to graphite nanoplatelets, have been decorated with metallic nanoparticles such as Pd and Pt to further increase electrocatalytic activity.[10−13] Results from such biosensors have been very promising, showing some of the best performances reported thus far, but a scalable fabrication technique is still lacking. Processes from exfoliation to random dispersion that limit control over the nanomaterial placement, as well as the nanoparticles' size and density, are currently used. Furthermore, these nanoparticle-decorated biosensors have limited biocompatibility and often require complex biofunctionalization schemes that increase fabrication time and cost.

Several techniques are available for decorating SWCNTs with metallic nanoparticles of various compositions. The most controllable and robust technique involves the electrodeposition of metal ions to defect sites on the nanotubes.[14,15] This bottom-up approach forms concentric metallic nanoparticles on the SWCNTs—nanoparticle size and density can be controlled by the electrodeposition potential, time, and metal salt concentration. A clear advantage of this electrochemical decoration is that the SWCNTs serve as both a template for nanoparticle growth and an inherent electrical contact to the nanoparticles for direct integration into devices. Recently, the ability to control the morphology, size, and density of electrodeposited Pd on SWCNTs was demonstrated, allowing for the formation of SWCNT networks decorated with uniform Pd nanocubes.[16] Additionally, alteration of the Pd nanocube surface by selective electrodeposition of a thin layer of Au has been demonstrated.[17]

Herein, we present a SWCNT-based electrochemical biosensor that utilizes Au-coated Pd (Au/Pd) nanocubes to enhance electrocatalytic activity, provide selective biofunctionalization docking points, and

*Address correspondence to tsfisher@purdue.edu.

Received for review October 14, 2008 and accepted December 15, 2008.

Published online January 5, 2009.
10.1021/nn800682m CCC: $40.75

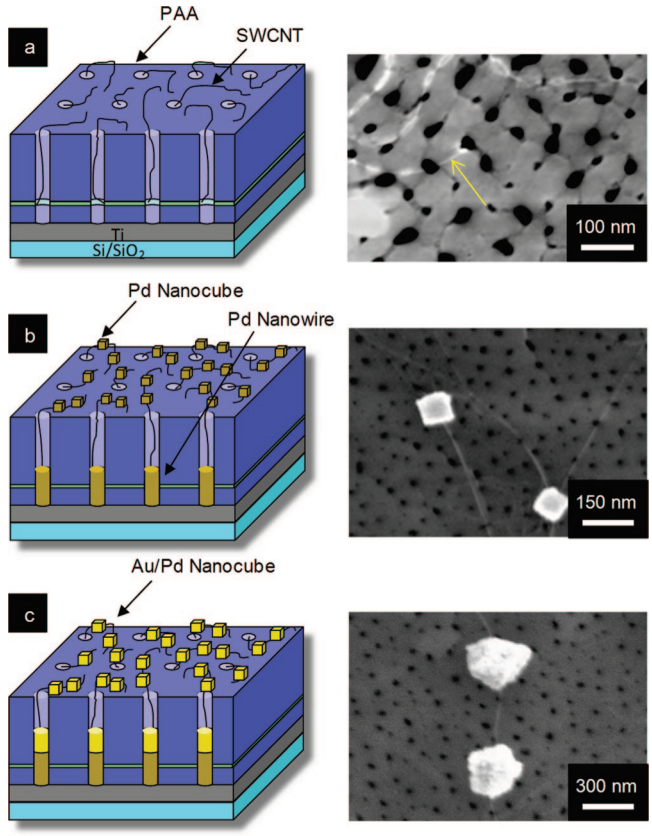

Figure 1. Tilted cross-sectional schematics with corresponding top-view field emission scanning electron microscopy (FESEM) micrographs portraying sequential fabrication process steps: (a) SWCNTs grown from the pores of the PAA via MPCVD (FESEM shows a SWCNT protruding from a pore and extending along the PAA surface), (b) electrodeposition of Pd to form Pd nanowires in pores and Pd nanocubes on SWCNTs (two such nanocubes are shown in corresponding FESEM), and (c) electrodeposition to coat the existing Pd nanocubes with a thin layer of Au.

improve biocompatibility. The biosensor exhibits specific and sensitive detection of a clinically important biomarker, glucose, with superior performance in comparison to other nanoscale biosensors that incorporate Au nanoparticles (AuNPs) and CNTs. Au/Pd nanocubes of homogeneous size and shape are integrated within an electrically contacted network of SWCNTs. The Pd provides a low-resistance contact between the SWCNT and Au interfaces,[18] while the Au provides the biocompatibility necessary for biofunctionalization, potentially with a myriad of ligands and other important biomarkers. Amperometric detection of hydrogen peroxide is used for preliminary characterization of the biosensor. To demonstrate an important medical application, the Au/Pd nanocubes are selectively immobilized with glucose oxidase (GOx) via thiol linking for amperometric glucose detection. Results reveal a high sensitivity, wide linear range, and low detection limit toward glucose. These results not only illustrate the effectiveness of the nanocube-SWCNT biosensor for glucose sensing, but they also prove the utility of the biosensor's microenvironment for immobilization with vast quantities of enzyme and excellent electron transfer between the enzyme and biosensing chip. An added advantage of these biosensors is that their fabrication is straightforward and easily scalable for integration into commercial biosensors with customized biofunctionalization for the detection of a desired molecular environment.

RESULTS AND DISCUSSION

Fabrication of Biosensors. The first step in the fabrication of the nanocube-SWCNT biosensors involves the fabrication of a porous anodic alumina (PAA) supporting template for SWCNT growth.[19] The PAA templates consist of pores with an average diameter and pitch of 20 and 100 nm, respectively. SWCNTs nucleate within the pores and grow vertically until they protrude from their pore and extend laterally along the PAA surface, creating a low density, interlacing network (Figure 1a). Previous reports have shown that low density SWCNT arrays, where individual tubes act as distinct nanoelectrodes, exhibit higher sensitivities and lower detection limits than macroscale carbon paste or SWCNT thin film electrodes.[20,21] The low density, horizontal portions of the SWCNTs on the PAA surface allow biomolecules to reach the SWCNT sidewalls unabated for detection and also permit controlled electrodeposition of metallic nanocubes on the SWCNT surfaces—a process that is not possible using dense forest-like SWCNTs in our experience. Furthermore, this facile *in situ* fabrication process allows for the attainment of controlled-density SWCNT networks,[22] whereas SWCNT thin film electrodes[10,23,24] and SWCNT paste electrodes[25−27] offer little density control and often include complex SWCNT processing steps.

To provide docking ports for enzymatic functionalization, Au/Pd nanocubes are electrodeposited onto the SWCNTs.[16,17] The nanocubes are produced by first electrodepositing Pd into the PAA, which forms Pd nanowires within the pores[28] that provide electrical contact to the SWCNTs, thus adding the SWCNTs to the electrochemical electrode and causing well-defined Pd nanocubes to form at the SWCNT defect sites (Figure 1b).[16,19] A low resistance contact is created at the SWCNT−Pd interface because of the high work function and wetting capabilities of Pd with SWCNTs.[18,29]

Following the fabrication of the Pd nanocube-decorated SWCNTs, Au is electrodeposited to provide a thin layer that coats the existing nanocubes (Figure 1c). This capping layer of Au, with its inherent resistance to oxidization and chemical fouling, creates an interface that is amenable to biofunctionalization with a wide range of biomarkers and chemical ligands. Furthermore, Au nanoparticles are advantageous for glucose sensing because they act as an electrocatalyst in the oxidation/reduction of H_2O_2,[30] are excellent electrical conductors,[31] and are hypothesized to promote direct electron transfer between the enzyme and electrode surface.[32,33]

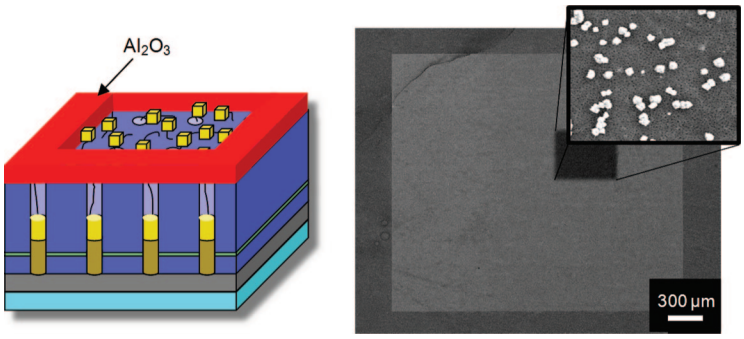

Figure 2. Tilted cross-sectional schematic and corresponding FESEM micrographs portraying deposited Al_2O_3 to define controlled electrode surface area. The FESEM micrograph shows lithographically patterned Al_2O_3 on the top surface of the nanocube-SWCNT electrode, with an inset showing a magnified view of Au/Pd nanocubes and SWCNTs on the PAA surface.

The final step for fabricating the nanocube-augmented SWCNT biosensors involves definition of the electrode area. Surface area definition is accomplished by lithographically patterning the nanocube-SWCNT electrode to protect the active region while Al_2O_3 is electron-beam evaporated to inactivate the remainder of the template as illustrated in Figure 2. Defining the surface area of the electrode enables variation of the sensitivity for optimization of the signal-to-noise ratio.[34]

Biofunctionalization of Nanocubes. To verify the biofunctionalization capability of the Au/Pd nanocubes, thiolated biotin ligands are coupled to the biosensor. The complementary protein of biotin, streptavidin, is subsequently fluorescently labeled and captured by the biotin-coupled Au/Pd nanocubes. Fluorescence microscopy is used to characterize the selective binding of fluorescently labeled streptavidin to the biotin-coupled Au/Pd nanocubes (Figure 3).

Hydrogen Peroxide Detection. To demonstrate the efficacy of the nanocube-SWCNT biosensor, hydrogen peroxide (H_2O_2) is used as a control system to perform several amperometric experiments *via* a three-electrode setup in 20 mL of phosphate buffer solution (PBS) at pH 7.4. The biosensor serves as the working electrode, a platinum wire as the auxiliary electrode, and a Ag/AgCl wire as the reference electrode. All tests involve detection of the redox current associated with the oxidation of peroxide at a working potential of 0.5 V and successive increases in concentration of 10 μM H_2O_2. A control experiment is run for comparison; a sample with bare SWCNTs in PAA with no decoration with Pd or Pd/Au nanocubes. As shown in Figure 4a, the bare SWCNT electrode experiences virtually no increase in current with each successive addition of H_2O_2.

In comparison to the bare SWCNT electrode, both of the nanocube-augmented electrodes exhibit significant increases in current associated with each successive addition of H_2O_2 and demonstrate linear regres-

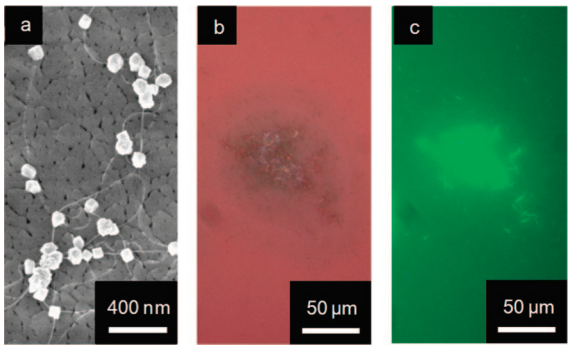

Figure 3. (a) High-magnification FESEM micrograph portraying a cluster of Au/Pd nanocubes connected by SWCNTs on the Au/Pd nanocube-SWCNT biosensor surface. (b) Optical micrograph portraying a large region of Au/Pd nanocube clusters and (c) fluorescence micrograph of the same region demonstrating the specific capture of Alexa-488 labeled streptavidin on the biotin functionalized Au/Pd nanocube clusters.

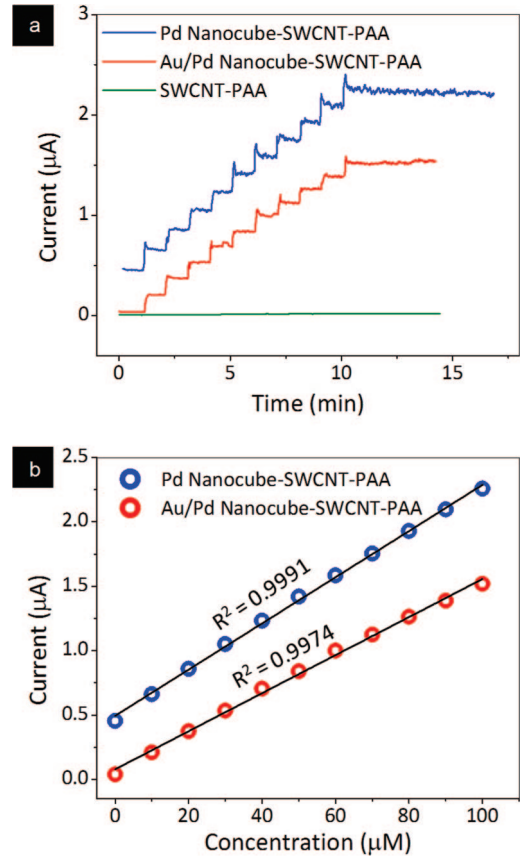

Figure 4. Amperometric sensing of H_2O_2 oxidation (0.5 V) in 20 mL of PBS (pH 7.4) using a three electrode potentiostat. The biosensor was tested by increasing the concentration of H_2O_2 by 10 mM (a) for the bare SWCNTs on PAA, Pd nanocube-SWCNT on PAA, and Au/Pd nanocube-SWCNT on PAA electrodes. The resulting data was processed and plotted as a scatter plot (current *vs* concentration) with linear regression analysis (b) for the Pd nanocube-SWCNT on PAA and the Au/Pd nanocube-SWCNT on PAA electrodes.

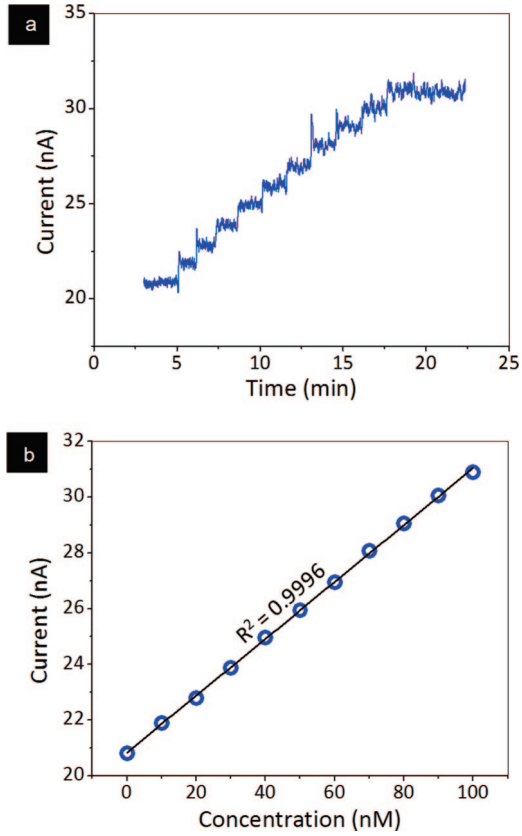

Figure 5. Amperometric hydrogen peroxide detection from a Au/Pd nanocube-SWCNT biosensor that has been pretreated in H_2SO_4 and NaOH. (a) Response in 20 mL of PBS (pH 7.4) with the biosensor polarized at a working potential of 0.5 V using a three electrode potentiostat. Successive additions of H_2O_2 aliquots increased the peroxide concentration by 10 nM. The resulting data was processed and plotted (b) as a scatter plot (current *vs* concentration) with linear regression analysis.

sions for H_2O_2 oxidation (Figure 4). The sensitivity of the Au/Pd nanocube-SWCNT electrode (370 μA mM^{-1} cm^{-2}) is slightly lower than the sensitivity of the Pd nanocube-SWCNT electrode (448 μA mM^{-1} cm^{-2}). This decrease in sensitivity confirms the enlargement of nanocube size by Au electrodeposition, which decreases the ratio of surface atoms with free valences to the cluster of total atoms, thus reducing sensitivity.[35,36] The SWCNTs of the bare SWCNT electrode are not electrically contacted to the underlying Ti conduction layer (Figure 1a) and therefore show little amperometric response to H_2O_2.

Electrochemical Pretreatment. To further increase sensitivity, the Au/Pd nanocube-SWCNT biosensor was electrochemically treated with 0.1 M H_2SO_4 at a potential scan that is cycled between 0 and 1.5 V with a scan rate of 100 mV/s for 25 cycles. The process is subsequently repeated with 0.1 M NaOH.[37] After these electrochemical pretreatments, the Au/Pd nanocube-SWCNT electrode consistently detects H_2O_2 concentrations as low as 10 nM with a sensitivity of 2.6 mA mM^{-1} cm^{-2} and a calculated detection limit of 2.3 nM (S/N = 3) (Figure 5). This H_2O_2 detection limit is 1−3 orders of magnitude lower than comparable SWCNT and colloidal Au nanoparticle-based amperometric biosensors.[38−40] We hypothesize that this increased electrocatalytic activity toward the oxidation of H_2O_2 is caused by the increase of defect sites and oxygenated species at the SWCNT sidewalls due to the 0.1 M H_2SO_4 and 0.1 M NaOH treatments, respectively. It has been reported that increased defect sites[41,42] and surface oxide species[43,44] greatly enhance the electron transport through the otherwise relatively inert SWCNT sidewalls.

Glucose Detection. Enzymatic glucose biosensors have been analyzed more than any other enzyme-based biosensor because of their vital role in blood glucose monitoring in diabetic patients. Typically, these GOx-based amperometric biosensors measure the glucose concentration by the electrocatalytic detection of hydrogen peroxide produced during the GOx/glucose reaction. The chemical reactions for this enzymatic breakdown of glucose *via* GOx along with the subsequent oxidation of hydrogen peroxide are as follows:

$$\text{D-glucose} + O_2 + H_2O \xrightarrow{\text{GOx}} \text{D-gluconicacid} + H_2O_2 \quad (1)$$

$$H_2O_2 \rightarrow 2H^+ + O_2 + 2e^- \quad (2)$$

To prepare samples for glucose sensing, GOx molecules are coupled to the Au/Pd nanocubes by a simple two-step biofunctionalization procedure illustrated in Figure 6. First, the Au/Pd nanocube-SWCNT electrode is incubated for 10 h in a thiol linker solution [dithiobis (succinimidyl undecanoate)] dissolved in tetrahyrdofuran (THF) (1 mg/mL), followed by rinsing with ultrapure water. During this incubation, the thiol linker molecules selectively attach to the Au surface on the nanocubes.[45] The thiol linker-bound chip is subsequently incubated with GOx [1 mg/ml in PBS (pH 7.4)] for 5 hours. This incubation causes the GOx enzymes to attach to the thiol linkers on the nanocubes. The GOx functionalized chip is triple-rinsed

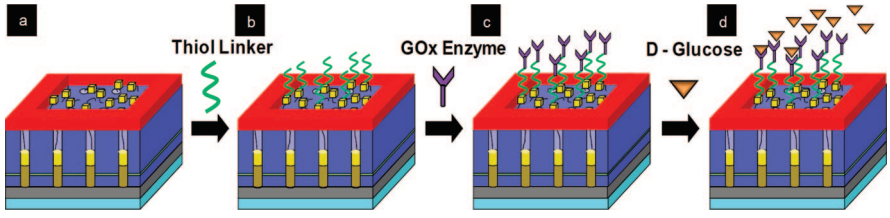

Figure 6. Tilted cross-sectional schematics illustrating electrode bioconjugation process steps: (a) a lithographically defined Au/Pd nanocube-SWCNT biosensor, (b) thiol covalent linking of dithiobis (succinimidyl undecanoate) to Au/Pd nanocubes, (c) covalent linking of GOx enzyme to thiol linker, and (d) attachment of D-glucose molecules to selective GOx sites.

with ultrapure water before amperometric glucose sensing.

Glucose sensing was accomplished with the same electroanalytical procedures used in the control experiments with hydrogen peroxide. The H_2O_2 generated from the enzymatic reaction of GOx and D-glucose is oxidized at the conductive SWCNTs and Au/Pd nanocube surfaces, producing a redox current that is proportional to the glucose concentration. The Au/Pd nanocube-SWCNT biosensor with a lithographically defined area of 0.04 cm^2 exhibits a highly linear glucose sensing range extending from 10 μM to 50 mM with a response time ~6 s (Figure 7a,b). After the electrochemical treatment mentioned heretofore, 10 μM glucose concentration increments were successively detected at a sensitivity of 5.2 μA mM^{-1} cm^{-2} and an estimated glucose detection limit of 1.3 μM (S/N = 3) (Figure 7c). This wide linear range and low detection limit indicates that the Au/Pd nanocube surface has a high capacity to immobilize active GOx.

Comparison to Similar Glucose Biosensors. As summarized in 1, the Au/Pd nanocube-SWCNT electrode outperforms comparable amperometric glucose biosensors based on AuNPs,[46,47] aligned SWCNT arrays,[20,24] Au-MWCNT arrays,[48] and Au nanowires[49] (AuNWs) in terms of detection limit, linear range, and response time. In particular, the detection limit of the Au/Pd nanocube-SWCNT biosensor is significantly lower and the linear range is higher than similar CNT and AuNP-based glucose biosensors (1). This performance enhancement can be attributed to a number of factors, including the controlled highly sensitive surface area, the low electrical resistance pathway at the nanocube-SWCNT interface, and the selective enzyme adhesion, activity, and electron transfer that occurs between the enzyme/Au/Pd nanocube interfaces. Whereas the compared SWCNT, AuNP, and Au nanowire-based glucose biosensors, utilize adsorption techniques[24,47−49] and covalent linking to SWCNTs[20] and AuNPs[46] to immobilize enzymes onto the electrode interface.

An additional advantage of the Au/Pd nanocube−SWCNT biosensor is the ability to control the size and density of the nanocubes that decorate the SWCNTs.[16] Optimizing the nanocube size and density for enzyme loading can produce a maximized amperometric output signal. Other reported SWCNT−Au nanoparticle electrodes rely on nanoparticle adsorption or chemical linking techniques in which nanoparticle size, density, and SWCNT/nanoparticle adhesion vary widely.[38,39,50,51] Another benefit is the small size and high surface area of the Au/Pd nanocubes, which enhances the performance of the biosensor in the peroxide oxidation process. The extremely low detection limit and linear range extending over 4 orders of magnitude implies that the immobilized GOx is highly active, indicating that the electrode provides a microenvironment suitable for the tertiary structure of the enzyme

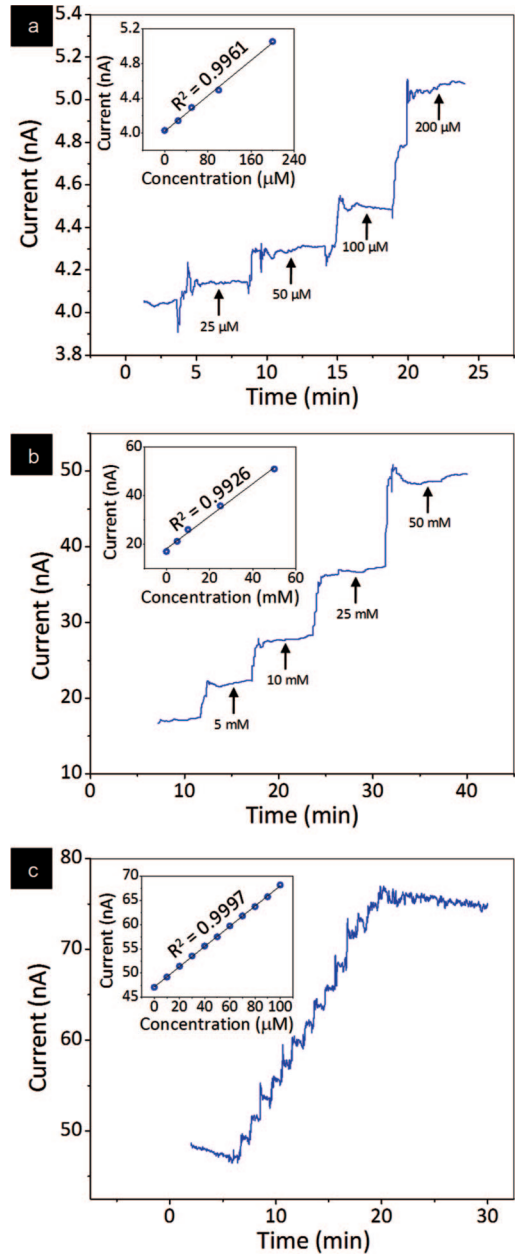

Figure 7. Electrochemically coupled glucose biosensor calibration experiment in 20 mL of PBS (pH 7.4). The biosensor is polarized to a working potential of 0.5 V and additions of glucose were added sequentially. Different concentration increases are used in the three representative calibrations including labeled concentration increases from (a) 25−200 uM increments and (b) 10−50 mM increments. (c) A biosensor that has been pretreated with H_2SO_4 and NaOH is calibrated by adding glucose concentrations in increments of 10 uM. The insets show the linear regression analysis of the current *vs* concentration profiles for each of the experiments.

while providing a low resistance pathway for glucose diffusion and subsequent oxidation of peroxide close to the electrochemical gold surface.

CONCLUSIONS

In conclusion, Au/Pd nanocubes were grown at the defect sites of templated SWCNT networks through a simple electrodeposition process. By altering the elec-

TABLE 1. Performance Comparison of CNT, Au Metallic Nanoparticle, And Au Nanowire Electrochemical Glucose Biosensors[a]

electrode description	detection limit [μM]	sensitivity [μA mM^{-1} cm^{-2}]	linear range [mM]	response time [s]	reference
Gox/Pd−Au/ASWCNTs/Si	1.3	5.2	0.01−50	6	this work
Au/cystamine/GOx	8.2	8.8	0.02−5.7	8	46
Nafion/GOx-GNPs/GCE	34	6.5	up to 6	15	47
Gox/ASCWNTs/Si	80	—	up to 30	20−30	20
SWCNTs/GCE	50	62	0.1−5.5	—	24
Au/MWCNT-Gox	10	—	0.05−0.13	16	48
Gox/AuNWs-Chitosan	5.0	—	0.01−10	8	49

[a]The dashes in the columns represent values that were not reported in the respective references.

trodeposition current, time, and metal salt concentration the size and morphology of the Au/Pd nanocubes could be controlled. The *in situ* fabrication of Au/Pd nanocubes on as-grown SWCNTs eliminates the need for complicated sorting, washing, and postprocessing required for most SWCNT-electrode immobilization schemes. Fluorescently labeled streptavidin was successfully bound to thiolated biotin ligands that were selectively immobilized on the Au/Pd nanocube surfaces, demonstrating the nanocubes ability to be biofunctionalized with covalent thiol linking schemes. The nanocube-augmented SWCNT biosensor effectively sensed successive increases of 10 nM H_2O_2 with a calculated current density of 2.6 mA mM^{-1} cm^{-2}. This high sensitivity toward H_2O_2 makes the biosensor an excellent platform for oxidase-based biosensing. The electrode was demonstrated as a glucose biosensor by immobilizing GOx on the surface of the nanocubes *via* thiol linking. Amperometric glucose sensing revealed that the nanocube-augmented SWCNTs outperformed similar SWCNT and metallic nanoparticle-based biosensors in terms of glucose detection limit, linear range, and response time. These promising results, combined with the biocompatibility of Au/Pd nanocubes, make this biosensor an exceptional choice for a wide range of biofunctionalization schemes and biomarker detection strategies. We also believe that the performance of this approach is sufficient for adaptation to a microbiosensor format[52] that could be used as a tool for biomedical research in single-cell biosensing applications.

METHODS

Reagents. PBS (0.1 M pH 7.4) was obtained from Invitrogen Corporation. Invitrogen. Dithiobis (succinimidyl undecanoate) (10 mg, stored at 4 °C) was obtained from Dojindo Molecular Technologies, Inc. GOx (*Aspergillus niger* lyophilized powder, 100000−250000 units/g, stored at 20 °C), H_2O_2 (30% (w/w) in H_2O, stored at 4 °C), tetrahydorfuran (THF) (anhydrous >99.9% inhibitor free), palladium chloride (99.999% purity, 500 mg), and gold(III) chloride hydrate (99.999% purity, 500 mg) were obtained from Sigma Aldrich. Biotinylated PEG alkanethiol (25 mg, stored at 4 °C) was obtained from Senso Path Technologies. Fluorescently labeled streptavidin (21832 Streptavidin Dylight Alexa 488) and biotin linker (21341 EZ-Link Biotin HPDP) were obtained from Pierce Chemical Co. Oxalic acid dihydrate (ACS, 250 mg) was obtained from Alfa Aesar. Hydrochloric acid (HCL, 6 lb) which was added to the 2 mM $PdCl_2$ bath was obtained from J.T. Baker.

Synthesis of PAA Template for SWCNT Growth. A metal film stack consisting of consecutive metal layers of Ti (100nm), Al (100nm), Fe (1nm), and Al (400 nm) were thermally evaporated on an oxidized silicon wafer [P <100> Si (375nm), SiO_2 (100nm)] *via* a thermal evaporator (Veeco 7760). The underlying Ti metal layer serves two roles: (1) supplies the bottom electrode electrical contact and (2) acts as an adhesion layer for subsequent metal deposition. The Fe layer embedded within the Al metal layers supplies the catalytic nucleation point for SWCNTs. The metalized substrate was immersed in 0.3 M oxalic acid bath held at 5 °C and biased with 40 V *versus* a Pt gauze auxiliary electrode. This anodization process transforms the Al metal layers into the dielectric Al_2O_2, forming semiordered pores (20−30 nm in diameter) through the Al/Fe/Al metal layers known as porous anodic alumina (PAA) or anodic aluminum oxide (AAO). A portion of the substrate was not anodized, leaving an electrically conductive contact pad composed of the evaporated metals for subsequent electrodeposition and amperometric sensing.

Growth of SWCNTs on Electrode Surface. Electrically addressable individual SWCNTs are grown from an Fe layer embedded in the pores of the PAA through a microwave plasma enhanced chemical vapor deposition (MPCVD) reactor (SEKI AX5200S).[22] The anodized substrate was placed on a 5.1 cm diameter molybdenum puck and heated in a hydrogen ambient to 900 °C by a 3.5 kW radio frequency power supply. Once the sample reached 900 °C, a 5 kW ASTeX AX2100 microwave generator was powered to create an unbiased 300 W hydrogen plasma over the substrate. This hydrogen plasma serves a dual purpose, (1) it penetrates the oxide barrier at the base of the PAA pores and (2) it decomposes methane, which acts as a precursor for SWCNT growth. After hydrogen plasma formation, methane was introduced into the MPCVD for 10 min to achieve SWCNT growth. The SWCNTs extend vertically from the pores of the PAA eventually resting horizontally on the surface of the PAA itself and vary in length from 3−10 μm (Figure 1a).

Formation of Pd Nanocube-SWCNT Networks. Decoration of the SWCNTs with Pd was performed by a BASi Epsilon three-electrode cell stand. Pt gauze acted as the auxiliary electrode, a Ag/AgCl wire as the reference electrode, and the SWNCT/PAA substrate as the working electrode. Pd was galvanostatically electrodeposited on the SWCNT-PAA structure by applying 500 ms pulses of 2 mA/cm^2 current between the auxiliary and working electrode for 250 cycles in a 2 mM $PdCl_2$ bath. Pulse currents allow for the double layer to dissipate between cycles allowing for consistent and controlled Pd deposition in the pores and defect sites of the SWCNT-PAA templated structure. After Pd electrodeposition, the samples were rinsed in DI water and allowed to air-dry. The Pd electrodeposition serves two roles, (a) supplies the back contact to the SWCNTs by partially filling the pores of the PAA connecting the Ti bottom layer and Fe layer and (b) forms well-defined Pd nanocubes at SWCNT defect sites (Figure 1b).

Formation of Au/Pd Nanocube-SWCNT Networks. The SWCNTs were further decorated with Au through the use of the same BASi Ep-

silon cell stand and three-electrode setup.[17] The electrode was placed in a 15 mM $HAuCl_4$ bath and biased with 0.65 V *versus* a Pt gauze auxiliary electrode for 10 s. Constant voltage electrodeposition creates a diffusion limited Au deposition so Au deposition occurs only onto existing Pd and not on bare SWCNTs (Figure 1c). The Au thickness on the Pd was varied by adjusting the electrodeposition time, bias, and metal salt concentration.

Biosensor Surface Definition. The surface area of the Au/Pd nanocube-SWCNT electrode was controlled by photolithography. After electrochemical pretreatment the electrode was solvent cleaned with acetone and methanol and dried under a gentle stream of N_2 to clean and prepare the samples for photolithography. Various areas were lithographically defined (5 mm × 5 mm, 3 mm × 3 mm, 2.5 mm × 2.5 mm, 2 mm × 2 mm, 0.5 mm × 0.5 mm) for optimal amperometric sensitivity toward hydrogen peroxide and glucose sensing. A film of Al_2O_3 of thickness of 400 nm was subsequently deposited on each sample *via* a Leybold e-beam evaporator. A subsequent 1 h acetone soak was used to lift off the remaining photoresist, leaving a well-defined rectangular area of SWCNT-Pd/Au surrounded by an oxide dielectric, Al_2O_3.

Biofunctionalization Procedures. ***Fluorescent Streptavidin/Biotin Immobolization.*** The biosensor is soaked in biotinylated PEG alkanethiol solution (0.20 mg/mL in ultrapure water) for 2 h, followed by rinsing with ultrapure water and drying under a stream of nitrogen gas. Next, the biosensor is exposed to 40 μL of fluorescently labeled streptavidin solution (Alexa-488 coupled streptavidin) for 10 min. After this incubation period, the biosensor is rinsed thrice with PBS and once with ultrapure water to remove buffer salts, followed by drying with nitrogen gas.

GOx Enzyme Immobilization. The biosensor was placed in 1 mL of THF that includes 1 mg of disolved dithiobis (succinimidyl undecanoate) for approximately 10 h. The electrodes are then double rinsed with PBS (0.1 M, pH 7.4, Sigma Aldrich) and placed in a GOx solution containing 1 mg of GOx enzyme (lyophilized powder, 100000−250000 units/g, Sigma Aldrich) for every 1 mL of PBS for 5 hours. Electrodes were stored at 4 °C until electrochemical testing.

Electrochemical Measurement. Amperometric sensing of glucose and H_2O_2 was performed on a BASi Epsilon three-electrode cell stand. Pt gauze acted as the auxiliary electrode, Ag/AgCl as the reference electrode, and the Au/Pd nanocube-SWCNT biosensor as the working electrode. During electrochemical measurements electrons travel from the Au/Pd-SWCNT/solution interface and through the SWCNTs to the Pd nanowires that are electrically connected to the Ti layer. The Ti layer, in turn, forms the metal underlayer of the electrically conductive contact pad of the Au/Pd nanocube-SWCNT biosensor and accordingly permits electron transfer to the cell stand. All amperometric measurements were acquired in PBS (0.1 M pH 7.4) at an overvoltage of 0.5 V.

Sample Imaging. Both optical and fluorescence images were acquired on a E1000 upright microscope (Nikon, Tokyo, Japan), using a 40× 0.75 NA Plan Fluor lens (Nikon), with a Retiga Exi CCD camera (QImaging, Surrey, BC, Canada). Fluorescence images were aquired using the FITC cube and a mercury arc lamp as the light source. Optical images (reflected light images) were aquired using a beamsplitter cube and a halogen lamp as the light source. All FESEM micrographs were obtained from a Hitachi S-4800.

Acknowledgment. The authors gratefully acknowledge assistance from Percy Calvo-Marzal for electrochemistry insight and Jennie Sturgis and Ghanashyam Acharya for fluorescence microscopy support. We also are grateful for funding from The Lilly Foundation and the Laura Winkelman Davidson Memorial Fellowship from the School of Mechanical Engineering of Purdue University.

REFERENCES AND NOTES

1. Drummond, T. G. Electrochemical DNA Sensors. *Nat. Biotechnol.* **2003**, *21*, 1192.
2. Patolsky, F.; Zheng, G.; Lieber, C. M. Nanowire Sensors for Medicine and the Life Sciences. *Nanomedicine.* **2006**, *1*, 51–65.
3. Hahm, J. i.; Lieber, C. M. Direct Ultrasensitive Electrical Detection of DNA and DNA Sequence Variations Using Nanowire Nanosensors. *Nano Lett.* **2004**, *4*, 51–54.
4. Wang, J. Portable Electrochemical Systems. *Trends Anal. Chem.* **2002**, *21*, 226–232.
5. Wang, J. Electrochemical Biosensors: Towards Point-of-Care Cancer Diagnostics. *Biosens. Bioelectron.* **2006**, *21*, 1887–1892.
6. Wilson, M. S. Electrochemical Immunosensors for the Simultaneous Detection of Two Tumor Markers. *Anal. Chem.* **2005**, *77*, 1496–1502.
7. Wang, J. Carbon-Nanotube Based Electrochemical Biosensors: A Review. *Electroanalysis.* **2005**, *17*, 7–14.
8. Cai, H.; Cao, X.; Jiang, Y.; He, P.; Fang, Y. Carbon Nanotube-Enhanced Electrochemical DNA Biosensor for DNA Hybridization Detection. *Anal. Bioanal. Chem.* **2003**, *375*, 287–293.
9. Yu, X.; Munge, B.; Patel, V.; Jensen, G.; Bhirde, A.; Gong, J. D.; Kime, S. N.; Gillespie, J.; Gutkind, S.; Papadimitrakopoulos, F.; Rusling, J. F. Carbon Nanotube Amplification Strategies for Highly Sensitive Immunodetection of Cancer Biomarkers. *J. Am. Chem. Soc.* **2006**, *128*, 11199–11205.
10. Hrapovic, S.; Liu, Y.; Male, K. B.; Luong, J. H. T. Electrochemical Biosensing Platforms Using Platinum Nanoparticles and Carbon Nanotubes. *Anal. Chem.* **2004**, *76*, 1083–1088.
11. Lim, S. H.; Wei, J.; Lin, J.; Li, Q.; KuaYou, J. A Glucose Biosensor Based on Electrodeposition of Palladium Nanoparticles and Glucose Oxidase onto Nafion-Solubilized Carbon Nanotube Electrode. *Biosens. Bioelectron.* **2005**, *20*, 2341–2346.
12. Lu, J.; Do, I.; Drzal, L. T.; Worden, R. M.; Lee, I. Nanometal-Decorated Exfoliated Graphite Nanoplatelet Based Glucose Biosensors with High Sensitivity and Fast Response. *ACS Nano.* **2008**, *2*, 1825–1832.
13. Tang, H.; Chen, J.; Yao, S.; Nie, L.; Deng, G.; Kuang, Y. Amperometric Glucose Biosensor Based on Adsorption of Glucose Oxidase at Platinum Nanoparticle-Modified Carbon Nanotube Electrode. *Anal. Biochem.* **2004**, *331*, 89–97.
14. Day, T. M.; Unwin, P. R.; Wilson, N. R.; Macpherson, J. V. Electrochemical Templating of Metal Nanoparticles and Nanowires on Single-Walled Carbon Nanotube Networks. *J. Am. Chem. Soc.* **2005**, *127*, 10639–10647.
15. Quinn, B. M.; Dekker, C.; Lemay, S. G. Electrodeposition of Noble Metal Nanoparticles on Carbon Nanotubes. *J. Am. Chem. Soc.* **2005**, *127*, 6146–6147.
16. Franklin, A.; Smith, J. T.; Sands, T. D.; Fisher, T.; Choi, K. S.; Janes, D. B. Controlled Decoration of Single-Walled Carbon Nanotubes with Pd Nanocubes. *J. Chem. Phys.* **2007**, *100*, 13756–13762.
17. Franklin, A. D.; Janes, D. B.; Claussen, J. C.; Fisher, T. S.; Sands, T. D. Independently Addressable Fields of Porous Anodic Alumina Embedded in SiO_2 on Si. *Appl. Phys. Lett.* **2008**, *92*, 013122.
18. Javey, A.; Guo, J.; Wang, Q.; Lundstrom, M. Ballistic Carbon Nanotube Field-Effect Transistors. *Nature* **2003**, *424*, 654–657.
19. Maschmann, M. R.; Franklin, A. D.; Scott, A.; Janes, D. B.; Sands, T. D.; Fisher, T. S. Lithography-Free *in Situ* Pd Contacts to Templated Single-Walled Carbon Nanotubes. *Nano Lett.* **2006**, *6*, 2712–2717.
20. Lin, Y.; Lu, F.; Tu, Y.; Ren, Z. Glucose Biosensors Based on Carbon Nanotube Nanoelectrode Ensembles. *Nano Lett.* **2004**, *4*, 191–195.
21. Tu, Y.; Lin, Y.; Ren, Z. F. Nanoelectrode Arrays Based on Low Site Density Aligned Carbon Nanotubes. *Nano Lett.* **2003**, *3*, 107–109.
22. Maschmann, M. R.; Franklin, A. D.; Sands, T. D.; Fisher, T. S. Optimization of Carbon Nanotube Synthesis from Porous Anodic Al−Fe−Al Templates. *Carbon* **2007**, *45*, 2290–2296.

23. Wang, L.; Wang, J.; Zhou, F. Direct Electrochemistry of Catalase at a Gold Electrode Modified with Single-Wall Carbon Nanotubes. *Electroanalysis* **2004**, *16*, 627–632.
24. Yao, Y.; Shiu, K. K. Electron-Transfer Properties of Different Carbon Nanotube Materials, and Their Use in Glucose Biosensors. *Anal. Bioanal. Chem.* **2007**, *387*, 303–309.
25. Gavalas, V. G.; Law, S. A.; Christopher Ball, J.; Andrews, R.; Bachas, L. G. Carbon Nanotube Aqueous Sol-Gel Composites: Enzyme-Friendly Platforms for the Development of Stable Biosensors. *Anal. Biochem.* **2004**, *329*, 247–252.
26. Rubianes, M. D.; Rivas, G. A. Carbon Nanotubes Paste Electrode. *Electrochem. Commun.* **2003**, *5*, 689–694.
27. Wang, J.; Musameh, M. Carbon Nanotube/Teflon Composite Electrochemical Sensors and Biosensors. *Anal. Chem.* **2003**, *75*, 2075–2079.
28. Franklin, A. D.; Maschmann, M. R.; DaSilva, M.; Janes, D. B.; Fisher, T. S.; Sands, T. D. In-Place Fabrication of Nanowire Electrode Arrays for Vertical Nanoelectronics on Si Substrates. *J. Vac. Sci. Technol., B.* **2007**, *25*, 343.
29. Ke, S. H.; Yang, W.; Baranger, H. U. Nanotube-Metal Junctions: 2-and 3-Terminal Electrical Transport. *J. Chem. Phys.* **2006**, *124*, 181102.
30. Bharathi, S.; Nogami, M. A Glucose Biosensor Based on Electrodeposited Biocomposites of Gold Nanoparticles and Glucose Oxidase Enzyme. *Analyst* **2001**, *126*, 1919–1922.
31. Eugenii Katz, I. W. J. W. Electroanalytical and Bioelectroanalytical Systems Based on Metal and Semiconductor Nanoparticles. *Electroanalysis* **2004**, *16*, 19–44.
32. Shipway, A. N.; M. L. I. W. Nanostructured Gold Colloid Electrodes. *Adv. Mater.* **2000**, *12*, 993–998.
33. Zhao, J.; Henkens, R. W.; Stonehuerner, J.; O'Daly, J. P.; Crumbliss, A. L. Direct Electron Transfer at Horseradish Peroxidase—Colloidal Gold Modified Electrodes. *J. Electroanal. Chem.* **1992**, *327*, 109–119.
34. Balasubramanian, K.; Burghard, M. Biosensors Based on Carbon Nanotubes. *Anal. Bioanal. Chem.* **2006**, *385*, 452–468.
35. Hrapovic, S.; Majid, E.; Liu, Y.; Male, K.; Luong, J. H. T. Metallic Nanoparticle-Carbon Nanotube Composites for Electrochemical Determination of Explosive Nitroaromatic Compounds. *Anal. Chem.* **2006**, *78*, 5504–5512.
36. Rao, C. N. R.; Kulkarni, G. U.; Thomas, P. J.; Edwards, P. P. Metal Nanoparticles and Their Assemblies. *Chem. Soc. Rev.* **2000**, *29*, 27–35.
37. Yao, H.; Sun, Y.; Lin, X.; Tang, Y.; Huang, L. Electrochemical Characterization of Poly (Eriochrome Black T) Modified Glassy Carbon Electrode and Its Application to Simultaneous Determination of Dopamine, Ascorbic Acid and Uric Acid. *Electrochim. Acta* **2007**, *52*, 6165–6171.
38. Chen, S.; Yuan, R.; Chai, Y.; Zhang, L.; Wang, N.; Li, X. Amperometric Third-Generation Hydrogen Peroxide Biosensor Based on the Immobilization of Hemoglobin on Multiwall Carbon Nanotubes and Gold Colloidal Nanoparticles. *Biosens. Bioelectron.* **2007**, *22*, 1268–1274.
39. Liu, Y.; Wang, M.; Zhao, F.; Guo, Z.; Chen, H.; Dong, S. Direct Electron Transfer and Electrocatalysis of Microperoxidase Immobilized on Nanohybrid Film. *J. Electroanal. Chem.* **2005**, *581*, 1–10.
40. Xu, Q.; Mao, C.; Liu, N. N.; Zhu, J. J.; Sheng, J. Direct Electrochemistry of Horseradish Peroxidase Based on Biocompatible Carboxymethyl Chitosan−Gold Nanoparticle Nanocomposite. *Biosens. Bioelectron.* **2006**, *22*, 768–773.
41. Banks, C. E.; Compton, R. G. New Electrodes for Old: From Carbon Nanotubes to Edge Plane Pyrolytic Graphite. *Analyst* **2006**, *131*, 15–21.
42. Moore, R. R.; Banks, C. E.; Compton, R. G. Basal Plane Pyrolytic Graphite Modified Electrodes: Comparison of Carbon Nanotubes and Graphite Powder as Electrocatalysts. *Anal. Chem.* **2004**, *76*, 2677–2682.
43. Li, J. Novel Three-Dimensional Electrodes: Electrochemical Properties of Carbon Nanotube Ensembles. *J. Phys. Chem. B* **2002**, *106*, 9299–9305.
44. Liu, J.; Chou, A.; Rahmat, W.; Paddon-Row, M. N.; Gooding, J. J. Achieving Direct Electrical Connection to Glucose Oxidase Using Aligned Single Walled Carbon Nanotube Arrays. *Electroanalysis* **2005**, *17*, 38–46.
45. Ferretti, S.; Paynter, S.; Russell, D. A.; Sapsford, K. E.; Richardson, D. J. Self-Assembled Monolayers: A Versatile Tool for the Formulation of Bio-Surfaces. *Trends Anal. Chem.* **2000**, *19*, 530–540.
46. Zhang, S.; Wang, N.; Yu, H.; Niu, Y.; Sun, C. Covalent Attachment of Glucose Oxidase to an Au Electrode Modified with Gold Nanoparticles for Use as Glucose Biosensor. *Bioelectrochemistry.* **2005**, *67*, 15–22.
47. Zhao, S.; Zhang, K.; Bai, Y.; Yang, W.; Sun, C. Glucose Oxidase/Colloidal Gold Nanoparticles Immobilized in Nafion Film on Glassy Carbon Electrode: Direct Electron Transfer and Electrocatalysis. *Bioelectrochemistry* **2006**, *69*, 158–163.
48. Wang, S. G.; Zhang, Q.; Wang, R.; Yoon, S. F.; Ahn, J.; Yang, D. J.; Tian, J. Z.; Li, J. Q.; Zhou, Q. Multi-Walled Carbon Nanotubes for the Immobilization of Enzyme in Glucose Biosensors. *Electrochem. Commun.* **2003**, *5*, 800–803.
49. Lu, Y.; Yang, M.; Qu, F.; Shen, G.; Yu, R. Enzyme-Functionalized Gold Nanowires for the Fabrication of Biosensors. *Bioelectrochemistry* **2007**, *71*, 211–216.
50. Liu, L.; Wang, T.; Li, J.; Guo, Z.-X.; Dai, L.; Zhang, D.; Zhu, D. Self-Assembly of Gold Nanoparticles to Carbon Nanotubes Using a Thiol-Terminated Pyrene as Interlinker. *Chem. Phys. Lett.* **2003**, *367*, 747–752.
51. Wang, S. G.; Zhang, Q.; Wang, R.; Yoon, S. F. A Novel Multi-Walled Carbon Nanotube-Based Biosensor for Glucose Detection. *Biochem. Biophys. Res. Commun.* **2003**, *311*, 572–576.
52. Porterfield, D. M. Measuring Metabolism and Biophysical Flux in the Tissue, Cellular and Sub-Cellular Domains: Recent Developments in Self-Referencing Amperometry for Physiological Sensing. *Biosens. Bioelectron.* **2007**, *22*, 1186–1196.